

PACS numbers: 81.15.Pq, 81.16.Be, 81.65.Cf, 82.45.Mp, 82.45.Qr, 82.45.Yz, 82.47.Wx

## **Investigation of the Dynamics of Electrochemical Dissolution of $n$ -InP(111) in Various Electrolyte Compositions and Determination of Optimal Etching Conditions**

Yana Sychikova<sup>1</sup>, Sergii Kovachov<sup>1</sup>, Ihor Bohdanov<sup>1</sup>, Ivan Kosogov<sup>1</sup>,  
Daria Drozhcha<sup>1</sup>, Zhakyp T. Karipbayev<sup>2</sup>, and Anatoli I. Popov<sup>3</sup>

<sup>1</sup>*Berdyansk State Pedagogical University,  
4, Schmidta Str.,  
71100 Berdyansk, Ukraine*

<sup>2</sup>*L. N. Gumilyov Eurasian National University,  
2, Satpayev Str.,  
KZ-010008, Kazakhstan*

<sup>3</sup>*Institute of Solid State Physics,  
University of Latvia,  
8, Kengaraga Str.,  
1063 Riga, Latvia*

We present a study on the dynamics of the electrochemical dissolution of  $n$ -InP(111), explicitly analysing the behaviour of the ‘electrolyte–semiconductor’ system in different electrolyte compositions, based on the analysis of critical points of the electrochemical reaction. Critical points are defined as characteristics of the technological process, where active phase dissolution of the sample surface is observed. We determine the minimum and maximum current-density values required to initiate the pore formation process on the surface of  $n$ -InP(111) in different electrolyte compositions. Additionally, for all cases, the duration of the active phase of surface dissolution and the Flade’s potential values are determined. This allows us to establish optimal parameters for treatment time, current density, and anodizing voltage for etching  $n$ -InP(111) in aqueous and alcoholic solutions of hydrochloric, hydrofluoric, and nitric acids. This, in turn, enables understanding and investigation of the kinetics of electrochemical surface dissolution as an essential result for unifying the requirements of the technological process of nanostructuring the surface of indium phosphide. The tools presented for analysing the dynamics of the electrochemical dissolution of  $n$ -InP can be applied to assess the behaviour of various semiconductors during electrochemical etching.

Представлено результати дослідження динаміки електрохімічного розчинення  $n$ -InP(111) на підґрунті аналізу поведінки системи «електроліт–

напівпровідник» у різних композиціях електролітів із врахуванням критичних точок електрохімічної реакції. Критичні точки визначають як характеристики технологічного процесу, за яких спостерігається активне фазове розчинення поверхні зразка. Ми визначили мінімальне та максимальне значення густини струму, необхідні для ініціювання процесу пороутворення на поверхні *n*-InP(111) у різних композиціях електролітів. Додатково для всіх випадків визначено тривалість активної фази поверхневого розчинення та значення потенціалу Фладе. Це уможливило встановити оптимальні параметри часу оброблення, густини струму та напруги анодування для щавлення *n*-InP(111) у водяних і спиртових розчинах соляної, фтористоводневої й азотної кислот. Це, у свою чергу, дає змогу зрозуміти та дослідити кінетику електрохімічного розчинення поверхні, що є важливим результатом для уніфікації вимог технологічного процесу наноструктурування поверхні фосфіду Індію. Представлені нами інструменти для аналізу динаміки електрохімічного розчинення *n*-InP можуть бути застосовані для оцінки поведінки різних напівпровідників під час електрохімічного щавлення.

**Key words:** electrochemical etching, electrochemical reaction, electrolyte, Flade's potential, critical points, optimal conditions.

**Ключові слова:** електрохімічне щавлення, електрохімічна реакція, електроліт, потенціал Фладе, критичні точки, оптимальні умови.

*(Received 31 December, 2023)*

## 1. INTRODUCTION

In recent years, nanostructured semiconductors have been intensively replacing their monocrystalline counterparts. This is primarily due to the new functional properties acquired by the semiconductor after structuring its surface [1, 2]. For instance, porous layers have found widespread applications as materials for solar energy and supercapacitors [3, 4]. Structures containing quantum dots are actively used as sensors [5], and multilayer heterostructures exhibit excellent photocatalytic properties [6].

Among all the methods of synthesizing nanostructures on the surface of semiconductors, electrochemical processing methods of crystals are the most economical [7]. They are time-limited and do not require expensive equipment or complex conditions [8]. The main disadvantage of these methods remains the difficulty in reproducing experimental results and synthesizing nanostructures with predefined properties [9]. At the same time, stringent quality requirements are imposed on engineering nanomaterials today [10, 11]. Therefore, optimizing electrochemical etching and deposition processes is highly relevant and requires intensive research. The micromorphology of semiconductor surfaces is influenced by the pa-

rameters of the initial crystal (impurities, defects) [12, 13] and synthesis conditions (time, electrolyte composition, applied potential) [14, 15]. Manipulating the initial characteristics of the crystal is very difficult, while the conditions of synthesis during the electrochemical processing of crystals can be easily adjusted during the experiment.

In this work, we investigate the dynamics of electrochemical dissolution of the surface of indium phosphide in different electrolyte compositions, focusing on changes in current density during the electrochemical reaction. This, in turn, allows for a deeper understanding of the mechanisms occurring at the semiconductor/electrolyte interface. Such research is necessary, first and foremost, for establishing general approaches to the controlled synthesis of nanostructures with predefined properties.

## 2. EXPERIMENT AND MATERIALS

For the experiment, a set of uniform monocrystalline indium-phosphide samples grown by the Czochralski method was used. The InP single crystals were obtained at the Molecular Technology GmbH laboratory (Berlin). The characteristics of the samples are provided in Table 1. The samples were cut into ingots measuring  $1 \times 2 \times 0.5 \text{ cm}^3$  and polished on both sides to a mirror finish.

Before the experiment, the samples underwent multistage cleaning to remove the oxide layer and dust from the surface. This cleaning is necessary to eliminate the influence of the surface state on the rate of the electrochemical dissolution reaction of the single crystal. The cleaning included the following stages:

1. step one: grinding the samples with M10 micro powder;
2. step two: mechanical polishing with ACM 3/2 diamond paste;
3. step three: chemical polishing in a 50% aqueous solution of a mixture of hydrochloric and perchloric acids ( $\text{HCl}:\text{HClO}_4 = 1:1$  by mass ratio);
4. step four: rinsing in isopropyl alcohol, acetone, and deionized

**TABLE 1.** The passport characteristics of InP samples used in the experiment.

Conduction type	$n$
Surface orientation type	(111)
Alloying impurity	S
Concentration of non-basic charge carriers	$2.3 \cdot 10^{-18} \text{ cm}^{-3}$
Crystal lattice	sphalerite

water. After cleaning and without contact with air, the samples were immersed in the electrolyte solution.

### 3. EXPERIMENTAL METHODOLOGY

Nanostructures on the surface of *n*-InP were formed using electrochemical etching in aqueous and alcoholic acid solutions. Six sets of electrolytes were used, prepared according to the following formulation (in mass ratios):

$$\text{HNO}_3:\text{H}_2\text{O} = 1:4, \quad (1)$$

$$\text{HNO}_3:\text{H}_2\text{O}:\text{C}_2\text{H}_5\text{OH} = 1:4:2, \quad (2)$$

$$\text{HF}:\text{H}_2\text{O} = 1:4, \quad (3)$$

$$\text{HF}:\text{H}_2\text{O}:\text{C}_2\text{H}_5\text{OH} = 1:4:1, \quad (4)$$

$$\text{HCl}:\text{H}_2\text{O} = 1:4, \quad (5)$$

$$\text{HCl}:\text{H}_2\text{O}:\text{C}_2\text{H}_5\text{OH} = 1:4:2. \quad (6)$$

For convenience, electrolytes containing only water and acid will be referred to as aqueous, and those with the addition of ethyl alcohol will be called alcoholic.

For the experiment, a standard three-electrode electrochemical cell was used. The cathode (Pt), anode (InP), and reference electrode (Cl–Ag) were immersed perpendicularly to the bottom of the cell. The cell was also equipped with a blowing module and a mixer to ensure the removal of reaction products from the sample surface and to eliminate bubbles that actively formed during the reaction on the semiconductor plate and platinum. Volt–ampere characteristics were recorded using the MTEch SPG-500S potentiostat.

The initial anodizing voltage was set at  $U_0 = 2$  V. The voltage was then increased every minute by 0.5 V. All samples were etched for 10 minutes. After that, the samples were kept in the same electrolyte solution for an additional 1 minute to stabilize the surface states. The experiment was conducted in daylight and at room temperature of the electrolyte.

### 4. RESULTS AND DISCUSSION

During the electrochemical dissolution of the InP surface, there is a sequential process of adsorption of the chemically active component of the electrolyte on the active centres of the surface and its interaction with the surface atoms of the semiconductor, which have broken bonds.

Without surface relief, local surface structural defects act as active centres. Atoms of doping and uncontrolled impurities in the near-surface layer also serve as active centres.

Usually, the process of electrochemical dissolution of the semiconductor surface includes the following stages:

1. stage one: diffusion of reacting ions of the electrolyte to the surface of the semiconductor;
2. stage two: the capture of electrolyte ions by surface atoms and the formation of surface complexes;
3. stage three: dissociation of activated complexes into the electrolyte solution.

In this process, alternative chemical reactions can occur, including:

oxidation of the semiconductor surface due to interaction with oxygen atoms;

formation of dense insoluble films;

electrodeposition of reaction products leads to the formation of islands and crystallites, among others. The processes occurring at the electrolyte/semiconductor interface determine the rate of the electrochemical reaction.

Figure 1 demonstrates the kinetics of current density change during the etching of indium phosphide in aqueous and alcoholic nitric acid solutions. It can be observed that etching in the aqueous electrolyte has a more uniform character while etching in the alcoholic solution shows a clear peak. This indicates that alcohol, in this case, acts as a catalyst for the reaction. It facilitates the more rapid removal of reaction products from the sample surface. The sharp decrease in current density after the sixth minute of etching in both electrolyte solutions indicates the completion of the active phase of

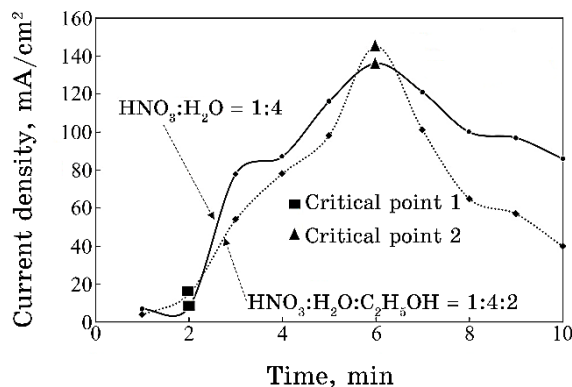


**Fig. 1.** Dependence of current density value on InP etching time for electrolyte solutions  $\text{HNO}_3:\text{H}_2\text{O} = 1:4$  and  $\text{HNO}_3:\text{H}_2\text{O}:\text{C}_2\text{H}_5\text{OH} = 1:4:2$ .

the dissolution of the semiconductor plate.

It should also be noted that for the electrochemical reaction in the aqueous nitric acid solution, a plateau of current density values is characteristic in the etching interval from 3 to 4 minutes. This suggests that in this solution, the samples were etched with the formation of an oxide film, which hindered active pore formation on the sample surface.

Indium phosphide demonstrates somewhat different behaviour when etched in hydrofluoric acid solutions (Fig. 2). It can be observed that the dynamics of current density change during the electrochemical reaction, exhibiting a 'staircase' pattern. This indicates the irregularity of etching on the indium phosphide surface. Such behaviour is characteristic of the electrochemical dissolution of *n*-

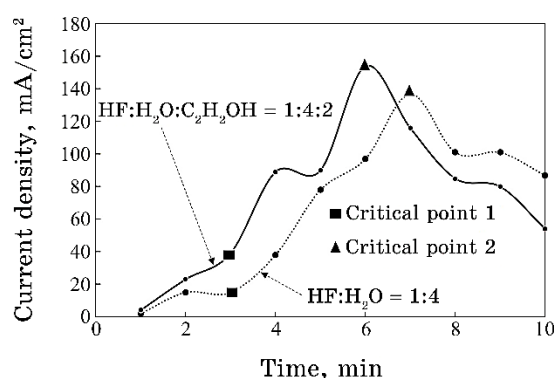


**Fig. 2.** Dependence of current density value on InP etching time for electrolyte solutions  $\text{HF}:\text{H}_2\text{O} = 1:4$  and  $\text{HF}:\text{H}_2\text{O}:\text{C}_2\text{H}_5\text{OH} = 1:4:2$ .

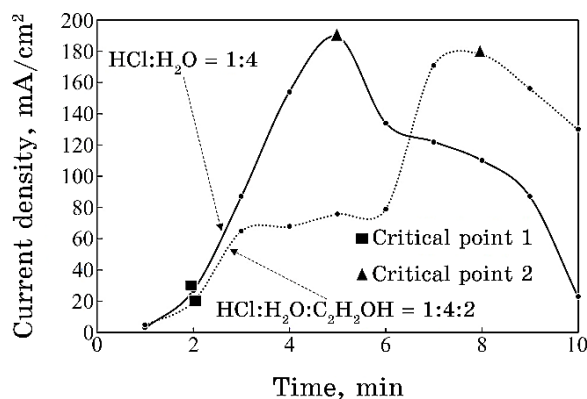


**Fig. 3.** Dependence of current density value on InP etching time for electrolyte solutions  $\text{HCl}:\text{H}_2\text{O} = 1:4$  and  $\text{HCl}:\text{H}_2\text{O}:\text{C}_2\text{H}_5\text{OH} = 1:4:2$ .

InP(111) in hydrofluoric acid solutions, a selective etchant. In this case, pores are initially etched at defect locations (defect-dislocation mechanism), and a bit later, chaotic etching of the surface begins (a seeding mechanism). This is more detailed in Ref. [16]. Figure 2 shows that the maximum current density value for the aqueous solution of hydrofluoric acid lags by 1 minute compared to etching in the alcoholic solution.

The case of etching *n*-InP(111) in hydrochloric acid solutions (Fig. 3) is interesting. Here, the maximum current density value when etching in the alcoholic HCl solution is delayed by three minutes compared to etching in the alcoholic solution. This suggests that for chlorine-containing electrolytes, alcohol acts as an inhibitor of the reaction. This is also indicated by the significant plateau of current density values in the interval from 3 to 6 minutes of etching. Most likely, the concentrations of hydrochloric acid at the given applied potential values are insufficient to initiate active pore formation on the surface of *n*-InP(111).

The maximum current density value corresponds to the Flade's potential ( $V_f$ ) value. Exceeding the value of  $V_f$  means that the InP surface oxidation rate becomes more significant than the dissolution rate. Figure 4 demonstrates the Flade's potential values for etching *n*-InP in all electrolyte compositions. The maximum value corresponds to the alcoholic hydrochloric acid solution, while the minimum is for the aqueous solution. Determining the Flade's potential is an essential step in optimizing the controlled synthesis of nanostructures with defined properties, and its value corresponds to the optimal potential to be applied for etching the crystal in a potentiostatic etching regime ( $U = \text{const}$ ).

Understanding the optimal duration of the reaction is also essential in describing the kinetics of electrochemical dissolution of the crystal. Figure 5 demonstrates the critical points of the beginning ( $t_1$ ) and end ( $t_2$ ) of the active phase of the electrochemical reaction in different electrolyte compositions, as well as the magnitude of  $\Delta t$ , which shows the duration of this phase and the difference between  $t_2$  and  $t_1$ . We can see that the start of the active phase corresponds to  $t_2 = 2$  min for chlorine and nitrogen-containing electrolytes. In contrast, the characteristic beginning of etching starts from the 3<sup>rd</sup> minute for hydrofluoric solutions. The most extended duration of the electrochemical reaction corresponds to the etching of *n*-InP(111) in the alcoholic hydrochloric acid solution. This may indicate uniform surface etching throughout the entire time with partial polishing. The duration of the active electrochemical reaction is an essential indicator of the electrochemical-process dynamics and determines the samples' optimal processing regime. The following formula should be used to determine the time required for

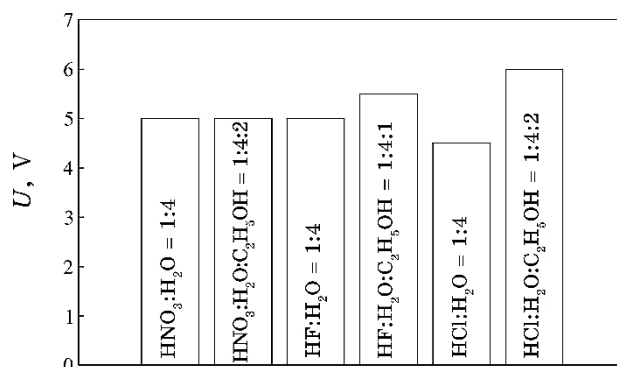


**Fig. 4.** Values of Flade's potential in electrochemical etching of *n*-InP in different electrolyte solutions.

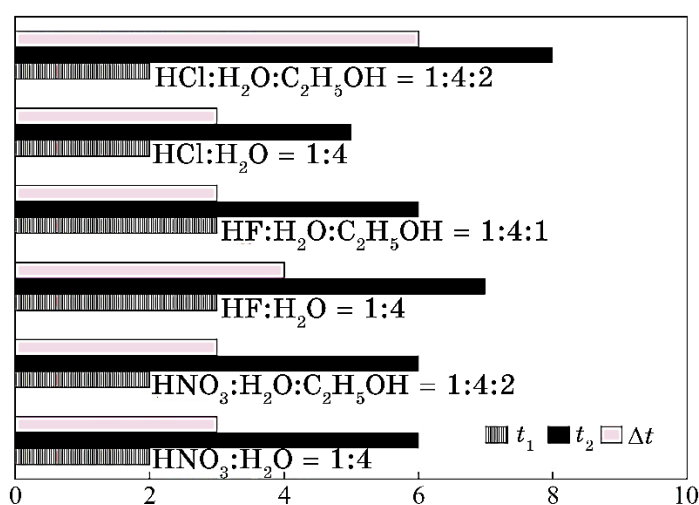


**Fig. 5.** Time diagrams of electrochemical treatment of *n*-InP samples in different electrolyte compositions.  $t_1$  is time of onset of the active phase of the electrochemical reaction;  $t_2$  is time of completion of the active phase of the electrochemical reaction;  $\Delta t = t_2 - t_1$  is term of active electrochemical reaction.

nanostructuring the surface:  $t_{opt} = \Delta t + 1$ . An additional minute is needed for the adsorption of electrolyte ions on the semiconductor surface at the initial stages of etching.

Determining the critical points of current density  $j_1$  and  $j_2$  allows us to define the permissible range of values for the active electrochemical dissolution reaction of the crystal. Current density values below  $j_1$  are insufficient to initiate the etching process while using  $j \gg j_1$  will lead to excessive etching of the sample and its destruc-

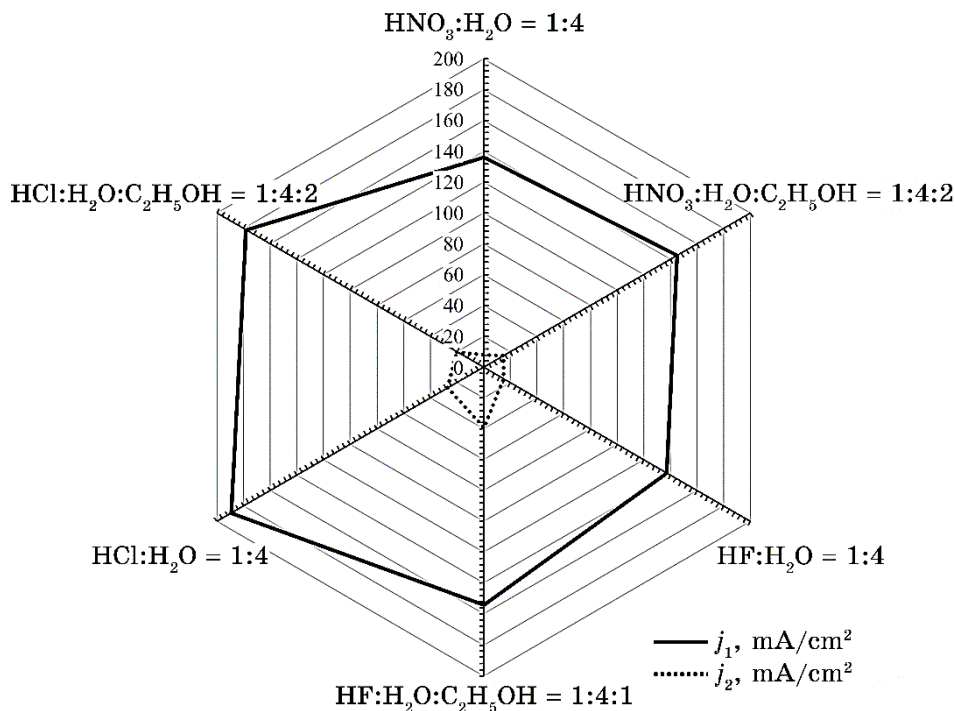


**Fig. 6.** The value of the critical points of the current density of electrochemical treatment of *n*-InP samples in different compositions of the electrolyte.  $j_1$  is current density at the beginning of the active phase of the electrochemical reaction;  $j_2$  is current density at the end of the active phase of the electrochemical reaction.

tion. Figure 6 demonstrates the values of critical points of current density for electrochemical processing of *n*-InP samples in different electrolyte compositions. It can be seen that the aqueous solution of nitric acid provides etching of the indium phosphide surface with the minimum current density value. This means that even without applied potential (chemical etching), moderately selective dissolution of the sample surface will occur. The highest value of  $j_2$  is characteristic of the aqueous solution of hydrochloric acid. This corresponds well with the results of determining the Flade's potential. Therefore, for etching *n*-InP(111), it is necessary to use regimes with high values of current density and anodizing voltage. This principle is used for evaluating other cases of etching.

Determining  $\Delta j = j_2 - j_1$  does not provide information about the optimal conditions for synthesis. Still, it is absorbing from the point of view of comparing the dynamics of the electrochemical process for different electrolyte compositions (Fig. 7).

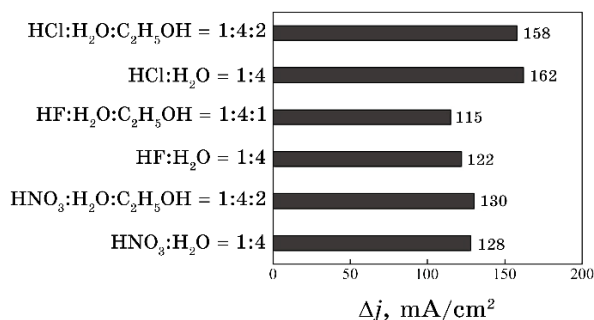


**Fig. 7.** The value of the parameter  $\Delta j$   $j_2$   $j_1$  in the electrochemical dissolution of  $n$ -InP in different compositions of the electrolyte.

For instance, the smallest value of  $\Delta j$  is characteristic of the alcoholic solution of hydrofluoric acid, indicating the need for precise adjustment of the electrochemical processing regimes in this electrolyte composition within a relatively narrow range of values. This is apparently due to the selectivity of this etchant and the two competing etching mechanisms (as described above). The highest value of  $\Delta j$  is characteristic of the aqueous solution of hydrochloric acid, which also confirms the earlier conclusion about the uniform etching of the  $n$ -InP(111) surface by the seeding pore formation mechanism. Optimal current density values will be found in the range  $[j_1; j_2]$ .

Summarizing the above observations, we can identify optimal etching regimes for  $n$ -InP(111) in potentiostatic and galvanostatic etching modes (Table 2).

The investigation and reasoning conducted above allow us to understand the mechanisms of the electrochemical dissolution of indium phosphide and to determine the critical values of the main char-

**TABLE 2.** Optimal etching modes for  $n$ -InP(111) in potentiostatic and galvanostatic etching regimes.

Electrolyte	Optimal modes of electrochemical dissolution		
	$t$ , min	$U$ , V under $U = \text{const}$	$j$ , mA/cm <sup>2</sup> under $j = \text{const}$
HNO <sub>3</sub> :H <sub>2</sub> O = 1:4	4	5	[8; 136]
HNO <sub>3</sub> :H <sub>2</sub> O:C <sub>2</sub> H <sub>5</sub> OH = 1:4:2	4	5	[15; 145]
HF:H <sub>2</sub> O = 1:4	5	5	[15; 137]
HF:H <sub>2</sub> O:C <sub>2</sub> H <sub>5</sub> OH = 1:4:1	4	5.5	[39; 154]
HCl:H <sub>2</sub> O = 1:4	4	4.5	[27; 189]
HCl:H <sub>2</sub> O:C <sub>2</sub> H <sub>5</sub> OH = 1:4:2	7	6	[20; 178]

acteristics of the process. This, in turn, provides a convenient tool for determining the optimal etching conditions for forming nanostructures with specified characteristics and unifying the requirements for the technological process.

## 5. CONCLUSIONS

The electrochemical dissolution of the surface of  $n$ -InP under an applied external potential is a complex physicochemical process that depends on many factors. An analysis of the dynamics of the electrochemical etching process of indium phosphide in aqueous and alcoholic solutions of hydrochloric, nitric, and hydrofluoric acids has been conducted.

The study of the dynamics of electrochemical dissolution of  $n$ -InP(111) in different electrolyte compositions allows us to make the following generalized conclusions.

There is a minimum and maximum value of the applied potential, at which an active dissolution reaction of the indium phosphide surface with microrelief formation on the surface will occur. These characteristics are selected for each case individually and depend primarily on the concentration and composition of the electrolyte.

To initiate the active phase of dissolution of the semiconductor surface, it is advisable to determine the Flade's potential, which corresponds to the maximum current density value and is defined as the optimal potential value to be applied for etching the crystal in a potentiostatic-etching mode. Determining the Flade's potential is essential in optimizing the controlled synthesis of nanostructures with defined properties.

The process of electrochemical dissolution of the crystal is limited in time. There are two critical time points characterizing the beginning and end of the active phase of the electrochemical dissolution reaction of the crystal surface.

At fixed values of the applied potential during the electrochemical etching of the indium phosphide surface, the electrolyte's composition will determine the current speed. This characteristic is determined separately for each case and allows in situ observation of the kinetics of the electrochemical process.

Based on the observations made on the dynamics of the electrochemical process and the obtained dependences, optimal etching regimes for  $n$ -InP(111) have been determined in potentiostatic and galvanostatic etching modes.

It should be noted that even slight deviations in the etching conditions could fundamentally change the optimal modes. This is due to several factors affecting the state of the 'electrolyte-semiconductor' system at each given moment.

## FUNDING

The study was supported by the Ministry of Education and Science of Ukraine *via* Project No. 0122U000129 ‘The search for optimal conditions for nanostructure synthesis on the surface of  $A_3B_5$ ,  $A_2B_6$  semiconductors and silicon for photonics and solar energy’. In addition, the research of A.P. and Y.S. was partly supported by COST Action CA20129 ‘Multiscale Irradiation and Chemistry Driven Processes and Related Technologies’ (MultiChem). A.P. thanks to the Institute of Solid State Physics, University of Latvia. ISSP UL as the Centre of Excellence is supported through the Framework Program for European universities, Union Horizon 2020, H2020-WIDESPREAD-01–2016–2017-TeamingPhase2, under Grant Agreement No. 739508, CAMART2 project.

## REFERENCES

1. I. Karbovnyk, B. Sadoviy, B. Turko, P. K. Khanna, and A. V. Kukhta, *Opt. Quantum Electron.*, **53**, No. 11: 647 (2021); <https://doi.org/10.1007/s11082-021-03292-1>
2. J. A. Suchikova, V. V. Kidalov, and G. A. Sukach, *ECS Trans.*, **25**, No. 24: 59 (2009); <https://doi.org/10.1149/1.3316113>
3. S. Kumar, G. Saeed, L. Zhu, K. N. Hui, N. H. Kim, and J. H. Lee, *Chem. Eng. J.*, **403**: 126352 (2021); <https://doi.org/10.1016/j.cej.2020.126352>
4. Y. O. Suchikova, I. T. Bogdanov, S. S. Kovachov, V. O. Myroshnychenko, and N. Y. Panova, *Arch. Mater. Sci. Eng.*, **101**, No. 1: 15 (2020); <https://doi.org/10.5604/01.3001.0013.9502>
5. M. J. Molaei, *Anal. Methods*, **12**, No. 10: 1266 (2020); <https://doi.org/10.1039/C9AY02696G>
6. R. B. Rajput, S. N. Jamble, and R. B. Kale, *J. Environ. Manage.*, **307**: 114533 (2022); <https://doi.org/10.1016/j.jenvman.2022.114533>
7. F. I. Danilov, D. A. Bogdanov, and V. S. Protsenko, *Vopr. Khim. Khim. Tekhnol.*, **2**: 3 (2022); <https://doi.org/10.32434/0321-4095-2022-141-2-3-8>
8. Y. S. Yana, *Handbook of Nanoelectrochemistry: Electrochem. Synth. Methods, Prop., Charact. Tech.*, 283 (2016); [https://doi.org/10.1007/978-3-319-15266-0\\_9](https://doi.org/10.1007/978-3-319-15266-0_9)
9. J. A. Suchikova, V. V. Kidalov, and G. A. Sukach, *Funct. Mater.*, **17**, No. 1: 131 (2010); J. A. Suchikova, V. V. Kidalov, and G. A. Sukach, *Semiconductors*, **45**, No. 1: 121 (2011); [doi:10.1134/S1063782611010192](https://doi.org/10.1134/S1063782611010192)
10. S. S. Kovachov, I. T. Bogdanov, D. O. Pimenov, V. V. Bondarenko, A. A. Konovalenko, and M. M. Skurska, *Arch. Mater. Sci. Eng.*, **110**, No. 1: 18 (2021); <https://doi.org/10.5604/01.3001.0015.3592>
11. C. Joseph Kennady, A. Leo, and P. Esther, *Vopr. Khim. Khim. Tekhnol.*, **2**: 17 (2022); <https://doi.org/10.32434/0321-4095-2022-141-2-17-23>
12. Abay Usseinov, Zhanymgul Koishybayeva, Alexander Platonenko, Vladimir Pankratov, Yana Suchikova, Abdirash Akilbekov, Maxim Zdorovets, Juris Purans, and Anatoli I. Popov, *Mater.*, **14**, No. 23: 7384 (2021);

- <https://doi.org/10.3390/ma14237384>
13. A. Usseinov, Z. Koishybayeva, A. Platonenko, A. Akilbekov, J. Purans, and V. Pankratov, *Latv. J. Phys. Tech. Sci.*, **58**, No. 2: 3 (2021);  
<https://doi.org/10.2478/lpts-2021-0007>
  14. Y. A. Suchikova, V. V. Kidalov, and G. A. Sukach, *J. Nano- Electron. Phys.*, **1**, No. 4: 78 (2009).
  15. Niankun Guo, Hui Xue, Amurisana Bao, Zihong Wang, Jing Sun, Tianshan Song, Xin Ge, Wei Zhang, Keke Huang, Feng He, and Qin Wang, *Angewandte Chemie*, **132**, No. 33: 13882 (2020);  
<https://doi.org/10.1002/ange.202002394>
  16. Y. A. Suchikova, V. V. Kidalov, and G. A. Sukach, *Semiconductors*, **45**, No. 1: 121 (2011); <https://doi.org/10.1134/S1063782611010192>